

Bacteriophage-mediated competition in *Bordetella* bacteria

Jaewook Joo^{*†}, Michelle Gunny^{*}, Marisa Cases^{*}, Peter Hudson[‡], Réka Albert[†], Eric Harvill^{*}

^{*}Department of Veterinary Science, [†]Department of Physics, [‡]Department of Biology,

Pennsylvania State University, University Park, PA 16802

(Dated: October 31, 2018)

ABSTRACT Apparent competition between species is believed to be one of the principle driving forces that structure ecological communities, although the precise mechanisms have yet to be characterized. Here we develop a model system that isolates phage-mediated interactions by neutralizing resource competition using two genetically identical *B. bronchiseptica* strains that differ only in that one is the carrier of a phage and the other is susceptible to the phage. We observe and quantify the competitive advantage of the bacterial strain bearing the prophage in both invading and in resisting invasion by bacteria susceptible to the phage, and use our measurements to develop a mathematical model of phage-mediated competition. The model predicts, and experimental evidence confirms, that the competitive advantage conferred by the phage depends only on the relative phage pathology and is independent of other phage and host parameters. This work combines experimental and mathematical approaches to the study of phage-driven competition, and provides an experimentally tested framework for evaluation of the effects of pathogens/parasites on interspecific competition.

INTRODUCTION Pathogen-induced damage to hosts, commonly observed as infectious disease, has been extensively investigated in humans and other animals [1, 2]. A pathogen can also confer a competitive advantage to one of two competing species through the process known as apparent competition [3, 4, 5, 6, 7, 8]. In both scenarios pathogens appear to drive the evolution of their hosts, exerting a selection pressure toward greater resistance [2, 3, 4, 9]. Increased resistance mechanisms of the hosts, including those as complex as the adaptive immune response of higher eukaryotes, does not seem to confer freedom from infection, but offers substantial advantage against other hosts more susceptible to the pathogen [9]. Pathogens are also driven to maximize their fitness (a function of virulence and transmission) although this is often a consequence of balancing virulence with transmission [10, 11]. Pathogen-mediated competition is an outcome of this ever-escalating arms race between the co-evolving hosts and pathogens.

There are a few excellent illustrative examples from the laboratory and field studies of ecological assemblage [3, 4, 5, 6] and even from the history of human diseases [12, 13]. However, due to the complexities originating from dynamical interactions among multiple-hosts and multiple-pathogens, it is not always easy to single out and quantitatively measure the effect of pathogen-mediated competition in nature. In a system of bacteria and bacteriophage it is relatively easy to manipulate

both host resistance mechanisms and pathogen virulence and thus this is one of the most suitable systems for the exploration of pathogen-mediated competition. In fact in recent studies [14, 15] laboratory communities of bacteria and lytic bacteriophage have been used as model systems for phage-mediated competition between phage-sensitive and phage-resistant bacteria. However, in these studies resource- and phage-mediated competitions were strongly intertwined and the role of one of the most important players in phage-mediated competition, lysogens (carriers of the phage), was not investigated.

To address these concerns in an examination of pathogen-mediated competition, we established an infection system using bacteriophage, neutralized resource competition by having two genetically identical strains and using large nutrient excess, and then examined competition between bacterial strains that differ only in their sensitivity to this phage. Particularly we used *Bordetella bronchiseptica*, a causative bacterium of mammalian respiratory disease, and its natural virus (BPP-1), a temperate phage that can either incorporate its DNA into the genome of *B. bronchiseptica* (lysogeny) or replicate itself and lyse the host bacterium (lysis). Here we demonstrate, both experimentally and theoretically, the existence of a competitive advantage conferred by this virus in a bacterial population, using a system in which this effect can be measured and quantified. Our results suggest that the lysogens are not only the source of phage during an infection process but can lead to fundamentally different dynamics in phage-mediated competition. We observe that the bacterial strain bearing the phage has an advantage in both invading and resisting invasion by bacteria susceptible to the phage and that the differential pathology on the two hosts is the sole variable that determines the quantitative value of phage-mediated competitive advantage. The theoretical representation of these interactions should have broad application to pathogen-mediated competition at many levels.

RESULTS The quantitative assessment of pathogen-conferred competitive advantage is usually hampered by the existence of direct competition over resources [3, 4, 5, 6]. To address this concern we use as our host populations *B. bronchiseptica* strains that are genetically identical except for defined genetic changes. The wild type parental *B. bronchiseptica* strain RB50 (Bb) was used to generate a strain (BbGm) that carries a gentamycin resistance marker shown not to affect expression of nearby genes and another (Bb:: ϕ) that is the carrier of, and is therefore resistant to, the temperate phage BPP-1 (ϕ) [16, 17]. To examine possible nutrient-dependent competition among

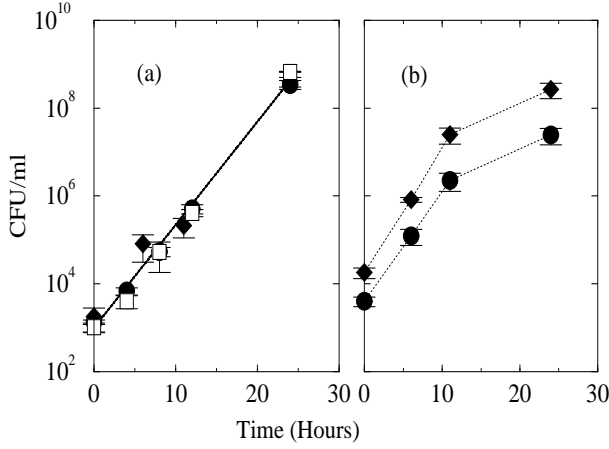


FIG. 1: The *in vitro* growth curves of *B. bronchiseptica* strains. (a) The three *B. bronchiseptica* strains, Bb:: ϕ (open squares), BbGm (filled circles) and Bb (filled diamonds) have identical growth curves when grown separately. The straight line corresponds to a doubling time of 77 minutes. (b) Bb and BbGm grow without competition when co-cultured.

these bacterial strains, we observed their *in vitro* growth rates. All three strains grew in nutrient rich medium with identical doubling time (77 minutes) over a range of cell densities from less than 1000 CFU/ml to over 10^9 CFU/ml (see Fig. 1). Bb and BbGm grew at the same rate when co-cultured, indicating that there is no effect of direct resource competition on their growth rates. The proportion of the final density of each strain was identical to the proportion at the start of the co-culture, indicating neutral competition between these two strains under these conditions.

We then examined phage-mediated competition using these *B. bronchiseptica* strains and the temperate bacteriophage BPP-1. The interactions involved in this system are schematically represented in Fig. 2. All bacterial strains divide with a constant rate a and bacterial populations grow with a density-dependent rate r . Susceptible bacteria (BbGm) become infected with a rate κ , defined as the number of contacts between a phage particle and a host bacterium per unit time multiplied by the probability of the host being infected upon contact. Upon infection the phage can take one of two pathways [18]. In a fraction P of infected BbGm, the phage replicate and then lyse the host after an incubation period $1/\lambda$, during which the bacteria do not divide [18]. Alternatively the phage lysogenize a fraction $1 - P$ of their hosts, incorporating their genome into that of the host. Thus the parameter P characterizes the pathogenicity of the phage, incorporating multiple aspects of phage-host interactions resulting in damage to host fitness. The lysogens (Bb:: ϕ and BbGm:: ϕ) carrying the prophage grow, replicating prophage as a part of the host chromosome, and are ϕ -resistant. Even though these lysogens are very stable [18] without external perturbations, spontaneous induction

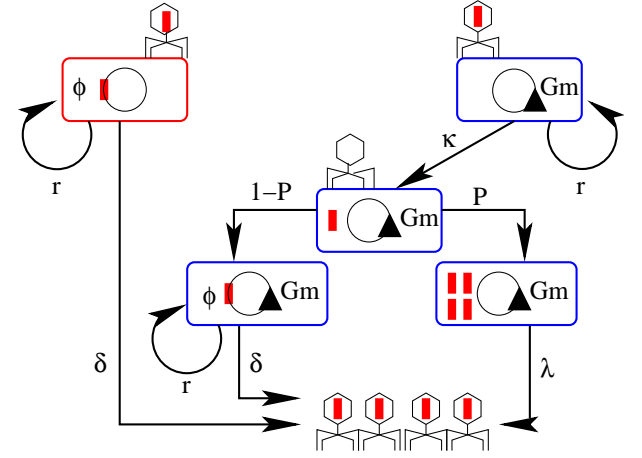


FIG. 2: Diagrammatic representation of phage-mediated competition between two bacterial strains. The phage (ϕ) is represented by a hexagon carrying a small thick line (ϕ DNA). Bacteria are represented by a rectangle containing an inner circle (bacterial DNA) while the bacterial strains bearing the prophage (Bb:: ϕ and BbGm:: ϕ) are represented by rectangles containing ϕ DNA integrated into bacterial DNA. Gm stands for gentamycin marker. All bacterial populations (Bb:: ϕ , BbGm and BbGm:: ϕ) grow with identical density-dependent growth rate r . Lysogens are spontaneously induced with a rate δ . The rate of a single bacterium being infected by a phage particle is given by the infection-causing contact rate κ . λ is the infection-induced lysis rate, and P the probability of the phage taking a lytic cycle. Resource is accessed and consumed by all bacteria.

can occur at a low rate δ , consequently replicating the phage and lysing the host bacteria. In general, both the number of phage produced (burst size) and the phage pathology P depend on the culture conditions [18]. This model predicts that when co-cultured, these two strains should compete through the phage, giving advantage to the lysogens.

To experimentally observe phage-mediated competition between two strains, Bb:: ϕ and BbGm were co-cultured *in vitro*. Since spontaneous induction of the phage from Bb:: ϕ is inevitable but would occur at variable time points (see Appendix B), we added a small number (1,000 PFU/ml) of exogenous phage to synchronously initiate phage-mediated competition. 1,000 CFU/ml of Bb:: ϕ and 1,000 PFU/ml of phage were added to a culture containing 10,000 CFU/ml of BbGm. As shown on Fig. 3(a), the total BbGm concentration (both susceptible BbGm and BbGm:: ϕ) increased with the same initial growth rate as Bb:: ϕ , but suddenly fell at about 8-12 hours postinfection. Within 24 hours the initial 1:10 ratio of Bb:: ϕ to BbGm was reversed to approximately 10:1, indicating a 100 fold relative increase in the proportion of Bb:: ϕ .

To observe the advantage of the lysogens in resisting invasion by the strain susceptible to the phage, 1,000 CFU/ml of BbGm was added to a culture containing

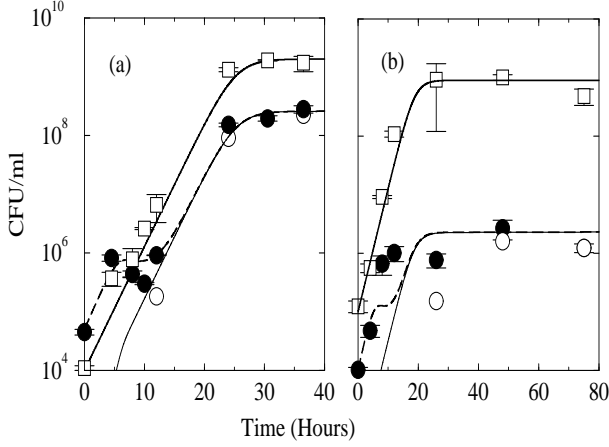


FIG. 3: *In vitro* experiments (symbols) and numerical simulations (lines) of (a) the invasion of the strain (Bb:: ϕ) exogenously and endogenously carrying the BPP-1 phage to the susceptible strain (BbGm), and (b) the protection of Bb:: ϕ against the invading BbGm. Symbols and lines represent Bb:: ϕ (open squares, thick solid line), BbGm:: ϕ (open circles, thin solid line), and the total BbGm (filled circles, long-dashed line), respectively. The parameters used for the numerical simulations are $\chi = 50$, $\alpha \equiv \delta/a = 0.1$, $\beta \equiv \lambda/a = 0.15$, $P = 0.98$. $\gamma \equiv S_B(0)\kappa/a = 0.01$ for (a) and $\gamma = 0.002$ for (b) where $S_B(0)$ is the initial concentration of BbGm.

10,000 CFU/ml of Bb:: ϕ and 10,000 PFU/ml of phage in Fig. 3(b). The initial 10:1 ratio of Bb:: ϕ to the total BbGm was amplified to approximately 1,000:1, indicating again a 100 fold increase in the proportion of Bb:: ϕ to the total BbGm.

We constructed a theoretical model of phage-mediated competition based on susceptible-infectious (SI) models describing the impact of directly transmitted pathogens on the dynamics of multiple hosts [19, 20, 21, 22, 23, 24]. We consider the dynamically interacting system of five subpopulations: (1) bacterial strain A (Bb:: ϕ) which bears the prophage and is thus resistant to the superinfection by the phage, bacterial strain B (BbGm) which can be in one of (2) susceptible, (3) latent, or (4) lysogenic states, and lastly (5) the bacteriophage (ϕ). Here a latent bacterium is one which is currently infected with the phage and will be lysed after the incubation period of the phage. We assume homogeneous mixing among all subpopulations, justified by vigorous stirring of the culture growth tube on an agitator. The time-evolution of each subpopulation is determined by the rates of incoming and outgoing flow in subpopulations, quantified by the rates given in Fig. 2. The five dimensional system of ordinary differential equations describing the bacteriophage-mediated competition is given by

$$\begin{aligned} \frac{dI_A(t)}{dt} &= (r(t) - \delta)I_A(t) \\ \frac{dS_B(t)}{dt} &= (r(t) - \kappa\Phi(t))S_B(t) \\ \frac{dL_B(t)}{dt} &= P\kappa\Phi(t)S_B(t) - \lambda L_B(t) \\ \frac{dI_B(t)}{dt} &= (1 - P)\kappa\Phi(t)S_B(t) + (r(t) - \delta)I_B(t) \\ \frac{d\Phi(t)}{dt} &= \chi(\delta(I_A(t) + I_B(t)) + \lambda L_B(t)) \\ &\quad - \kappa\Phi(t)S_B(t) \end{aligned} \quad (1)$$

where $I(t)$, $L(t)$ and $S(t)$ are the concentrations of the infected, latent and susceptible bacteria at time t , $N(t) = I_A(t) + I_B(t) + S_B(t) + L_B(t)$, $r(t) = a(1 - N(t)/N_{max})$ is the density-dependent growth rate of all bacteria, and N_{max} is the holding capacity, i.e. the concentration of bacteria supported by the nutrient broth environment. We directly measured the values of five parameters, a , δ , λ , χ and N_{max} , and estimate the others. The dimensions and relevant ranges of all parameters are given in Table I.

We compared the numerical simulation results with our experimental results for invasion and protection of the lysogens (Bb:: ϕ) carrying the phage in Fig. 3. The results validate our choice of theoretical model and parameters. We find that the experimentally determined and estimated values of parameters ($\chi = 50$, $\alpha \equiv \delta/a = 0.1$, $\beta \equiv \lambda/a = 0.15$, and the choice of $P = 0.98$ and $\gamma \equiv S_B(0)\kappa/a = 0.01$ [$\gamma = 0.002$]) lead to a good agreement with the experimental scenarios in Fig. 3(a) [3(b)], respectively. Minor discrepancies between experiments and simulations are noticeable in the time-evolution of the concentrations of BbGm:: ϕ and of the total BbGm. These are likely due to our assumption of homogeneous mixing of phage particles and bacterial hosts.

The success of our model in capturing the dynamic behavior of the bacteria-phage system in two different scenarios enables us to use it to determine the condition of a successful phage-mediated invasion and explore cases that are not addressed by experiments. We first investigated the invasion criterion, the choice of parameters in Table I which makes the invading strain A dominant in number over the invaded strain B. The condition of becoming the predominant organism depends only on the phage pathology P and on the initial ratio of the concentrations of bacterial strains A and B. We find that the final population ratio is approximately

$$r_{AB}(\infty) \simeq \frac{r_{AB}(0)}{1 - P}, \quad (2)$$

where $0 \leq P < 1$, $r_{AB}(\infty) = N_A(\infty)/N_B(\infty)$, $r_{AB}(0) = N_A(0)/N_B(0)$, and $N_A[N_B]$ is the total concentration of bacteria A[B] and $N_A(\infty) + N_B(\infty) = N_{max}$. In conclusion the invasion criterion (that is, the condition of

TABLE I: Parameters used for the numerical simulation of the phage-mediated competition in *B. bronchiseptica*. a [hours⁻¹] is determined from the measured doubling time (77 minutes) of Bb bacteria in mid-log phase in Fig. 1. λ [hours⁻¹] is determined from the observed phage incubation period (6-12 hours), which is the time-interval between initial contact of the phage particles with susceptible bacteria and bacterial lysis. χ is measured from the difference in the phage concentrations between 0 and 12 hours of ϕ and Bb co-culture. δ [hours⁻¹] is set to be 0.054 in our simulations. Note that we verified in Supporting Information that the invasion criterion in Eq. (3) remains valid for any $0 \leq \delta/a < 0.5$. The two undetermined parameters P and κ [[hours·CFU/ml]⁻¹] are estimated by comparing the experimental results with those of the theoretical model and by minimizing discrepancies.

Parameter	Name	Range	Resources
a	(Free) growth rate	0.54	measured
δ	Spontaneous lysis rate	$0 \leq \delta < a$	measured
λ	ϕ -induced lysis rate	0.08 - 0.17	measured
χ	Burst size	10 - 50	measured
P	Phage pathology	$0 \leq P \leq 1$	estimated
κ	Contact rate	$\kappa > 0$	estimated
N_{max}	Holding capacity	$\sim 10^9$	measured

$r_{AB}(\infty) > 1$) is

$$r_{AB}(0) > 1 - P. \quad (3)$$

The derivation of Eq. (2) was provided in Appendix in the limit $\gamma \gg 1$ ($\kappa S_B(0) \gg a$) and $\beta \gg 1$ ($\lambda \gg a$), that is, when susceptible bacteria are rapidly infected by phage particles and lysed immediately after infection. We also verified by extensive numerical simulations the validity of Eq. (2) in a much broader parameter range, especially for small γ and β .

The theoretical model predicts that different initial phage concentrations or different contact rates have no effect on the steady state outcome of the phage-mediated competition while either can modify the kinetics of the interactions (see the inset of Fig. 4). To validate its prediction of the model, we performed time course experiments with three different phage concentrations (see Fig. 4). The trajectories of the total BbGm population depend sensitively on the initial phage concentrations during the intermediate time-steps (between 0 and 24 hours), showing a larger fall of the total BbGm for higher phage concentration between 8 and 12 hours of co-culture. However the trajectories of Bb:: ϕ and the total BbGm converge to the same steady states within statistical errors after 48 hours regardless of initial phage concentration, indicating that the final outcome of phage-mediated competition does not depend on the initial phage concentration. This verifies the independence of the invasion criterion in Eq. (3) on the initial phage concentration and provides justification for the addition of exogenous phage to the system in Figs. 3(a) and 3(b).

We investigated the effect of the phage pathology on

the amount of the phage-mediated competition. We experimentally manipulated the phage pathology using a lytic phage ($\phi\Delta cI$) with an in-frame deletion in the cI repressor gene required for lysogeny [16, 17] that always lyses the host bacterium (and thus has $P = 1$). The lytic phage-mediated competition experiments shown on Fig. 5(a) clearly corroborate the numerical simulation. Co-culturing strains with this $\phi\Delta cI$ resulted in an approximately 1,000 fold advantage to the resistant strain (Bb:: ϕ) over the susceptible strain (BbGm). The small fraction of BbGm that survived appear to be ϕ -resistant due to infection by the wild type ϕ spontaneously released from Bb:: ϕ .

Finally we investigated one of several possible resistance mechanisms of bacteria against pathogenicity of the phage. A simple mutation can take place in the receptor complex of the host bacteria that renders them no longer susceptible to phage lacking the tropism switching mechanism. We used a mutant phage ($\phi\Delta orf5$) with in-frame deletion in the gene, *orf5*, encoding the reverse transcriptase necessary for the tropism switching mechanism. This phage can only infect bacteria bearing the protein pertactin. In Fig. 5(b) we co-cultured a bacterial strain with an in-frame deletion in the gene encoding pertactin (Bb Δprn Gm) with Bb:: $\phi\Delta orf5$ in the presence of 1000 PFU/ml of the mutant phage ($\phi\Delta orf5$) [16, 17, 25]. Both strains grow without any sign of phage-mediated

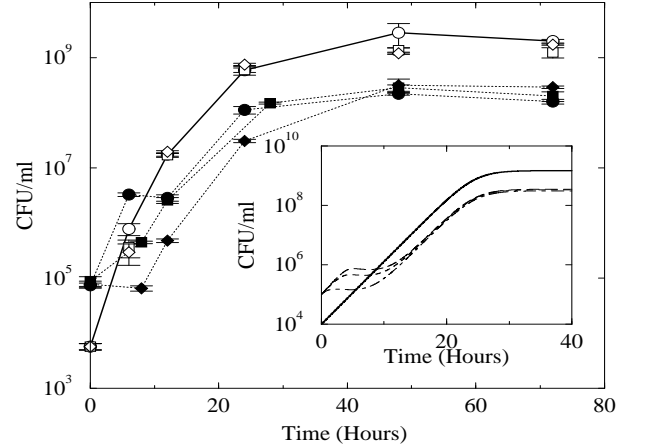


FIG. 4: Independence of the steady state outcome of phage-mediated competition on the initial phage concentration. Main: *In vitro* experiments of the time evolution of Bb:: ϕ (open symbols connected by a solid line) and the total BbGm (filled symbols, dotted lines) with initial exogenous phage concentrations of 10^1 (filled circles), 10^4 (filled squares) and 10^5 (filled diamonds) PFU/ml. Inset: Numerical simulations of the time evolution of Bb:: ϕ (solid line) and the total BbGm with three different initial phage concentrations of 10^1 (long-dashed line), 10^4 (dashed line) and 10^5 (dot-dashed line) PFU/ml. The parameters are $\chi = 50$, $\alpha = 0.1$, $\beta = 0.15$, $\gamma = 0.02$ and $P = 0.98$. Note that the numerical simulation results of the time-evolution of Bb:: ϕ and the total BbGm at different contact rates γ are similar to the pattern in the inset.

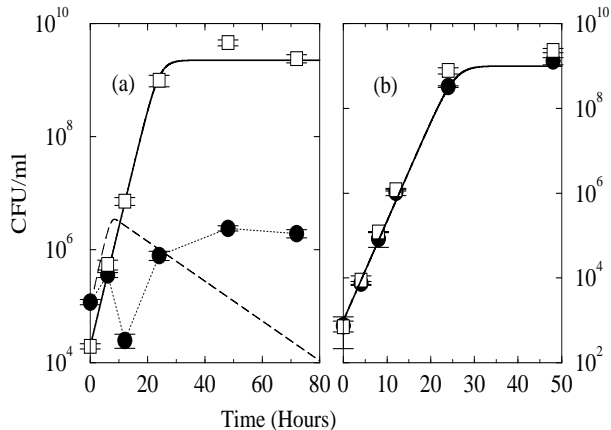


FIG. 5: Dependence of phage-mediated competition on the phage pathology P is observed in *in vitro* experiments (symbols) and numerical simulations (lines). Presented are time-evolutions of (a) the co-cultured Bb:: ϕ (open squares, solid line) and total BbGm (filled circles connected, dashed line) in the presence of exogenous lytic phage ($\phi\Delta cI$), and (b) the co-cultured Bb $\Delta prnGm$ (filled circles, solid line) and Bb:: $\phi\Delta orf5$ (open rectangles, dashed line) in the presence of mutant phage ($\phi\Delta orf5$). The parameters used for the numerical simulations are the same as in Fig. 3(a) except $\gamma = 0.01$ and $P = 1$ in (a) and $\gamma = 0$ (and thus $P = 0$) in (b).

competition and maintain the initial ratio for more than 24 hours.

DISCUSSION In most of the systems where pathogen-mediated competition has been observed, there have been confounding factors, such as different growth and reproductive rates of hosts, and intertwined resource and phage-mediated competitions, that have limited quantitative assessments of pathogen-mediated competition. The bacteria-phage system described here overcomes these difficulties to allow the accurate estimation of the parameters, in most cases directly measuring them experimentally. Understanding the impact of the pathogen pathology (the product of co-evolving pathogen virulence and host resistances against pathogens [2, 9, 26]) on pathogen-mediated competition requires a system in which both host defense mechanisms and pathogen pathology can be manipulated. Again bacteria and phage are suitable systems for these purposes.

We utilized *in vitro* experiments, analytical and numerical analysis to show the existence of bacteriophage-mediated competition between two host bacterial strains. In our *in vitro* experiments direct competition between host strains was minimized by using genetically identical strains and culture conditions that allow for unrestricted, exponential growth over many generations. The two bacterial strains differ only in the pathology of phage infecting them; the phage pathology (P) of the strain bearing the prophage (Bb:: ϕ) is almost zero while that of the susceptible BbGm is close to one. As we demonstrated here, the strain bearing the prophage has advantage in both

invading and resisting invasion by the phage-susceptible bacteria.

Our competition studies have revealed a single determining factor for competitive advantage. First, when the phage was manipulated to increase its pathology in the susceptible strain, the amount of competitive advantage conferred to the host carrying the prophage dramatically increased. Second, when both strains (Bb:: $\phi\Delta orf5$ and Bb $\Delta prnGm$) are resistant to phage ($\phi\Delta orf5$) infection, the phage didn't confer any competitive advantage to either strain. Third, we conjectured that none of the other details of the system contribute to the steady state outcome of phage-mediated competition between two strains, and we demonstrated experimentally the independence of the competition outcome on the initial concentration of the phage. Although different initial phage concentrations modified the kinetics of the interactions, they did not affect the final ratio of bacterial strains.

Our theoretical model captures the dynamical behavior of the bacteria-phage system and can be extended to predict the steady state outcome of phage-mediated competition under more general conditions. We demonstrated that when there is a quantitative difference in the resistance of the two bacterial strains, the success of the competing strains depends only on the ratio of the initial concentrations of two strains and the relative phage pathology. This conclusion leads to the following predictions for general pathogen-mediated invasion beyond bacteria-phage systems: a) For a pathogen to contribute to the ability of a host to invade an ecological niche requires that the pathogen pathology is lower in the invading population than in the invaded population. This is generally true when a disease endemic to one population is carried to populations that are naive to the disease. b) In the case of differential host resistance, one can conjecture that the final ratio of the two populations and the success of the invasion are determined by the following fraction,

$$r_{AB}(\infty) = r_{AB}(0) \frac{(1 - P_A)}{(1 - P_B)} \quad (4)$$

where $P_A[P_B]$ is the pathogen pathology. The condition for the success of the invasion of population A to population B is that $r_{AB}(\infty) \geq 1$. In Appendix we have verified the validity of the generalized invasion criterion by analytical and numerical analysis.

The above predictions can be naturally extended to pathogen-mediated invasion in nature if all the details of individual pathogen-host interactions can be condensed into a single parameter describing pathogen pathology. There are certain limitations to extrapolating the above conclusions to pathogen-mediated invasion in ecology and humans. First, the assumption that host populations and pathogens are well-mixed may be better suited *in vitro* than in nature. However, the theoretical models and experimental manipulation of phage concentrations suggest that the ultimate effect of pathogen-mediated

competition is not dependent on the rate of contact, and successful pathogens are, by their nature, very efficient at transmission (infection-causing contact). Second, the infection processes are discrete, stochastic and spatial in nature, and might not be completely described by differential equations. Third, pathogens can be transmitted without killing hosts in general infection processes, and the birth and death events in animal and human populations can be markedly different from bacterial growth. We expect that these differences will not have a major impact, though.

In conclusion our studies have important implications in relation to the long-term advantage of bearing multiple pathogens. An a priori view might have been that the heavier pathogen load might reduce fitness relative to a competitor. This view is directly contradicted by the findings of this study, in which the advantages of bearing a pathogen are clear and related to its relative pathology on the hosts. One further implication is that the relative advantage conferred by the pathogen to the host should be related to the length of time during which they have coexisted and co-evolved. Over time the pathogen will select for more resistant hosts, but will alter its own virulence to maintain optimal transmission and overall fitness. When that pathogen is introduced into a host population that has not been under that selection it will exhibit inappropriately high virulence. This effect is observed in, and potentially explains, zoonotic diseases that often cause more pathology in humans than in their naturally co-evolved host. Although each pathogen may moderate pathology to optimize reproduction in their new host, humans will continue to be assaulted by new pathogens with greater virulence.

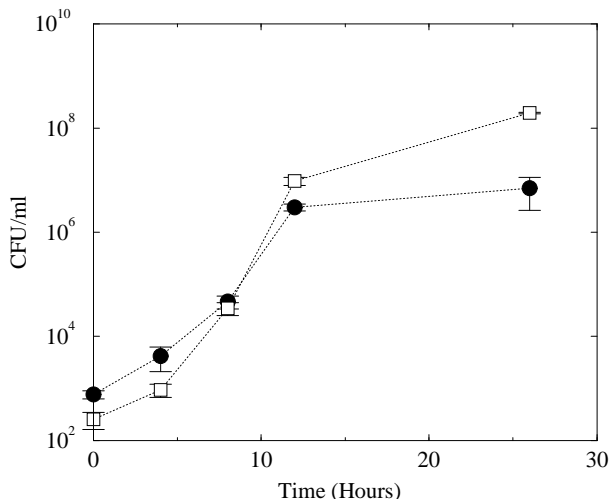


FIG. 6: *In vitro* evidence of the spontaneous release of phage. The strain carrying the phage (Bb:: ϕ , open squares) outnumbers the susceptible strain (BbGm, filled circles) without initial exogenous phage.

APPENDIX A: EXPERIMENTAL METHODS

A temperate bacteriophage BPP-1 and a mutant, which lacks the reverse transcriptase necessary for the tropism switching mechanisms and can only infect *B. bronchiseptica* bacteria bearing the protein pertactin BPP-1 $\Delta orf5$, were the kind gift of Jeff Miller [16, 17, 25].

B. bronchiseptica strains were grown on Bordet-Gengou (BG) agar plate, and incubated for three days at 37°C. Then 2-3 colonies of each strain were inoculated in 4 ml of Stainer Sholte media with supplements, and grown at 37°C overnight to mid log phase. For co-culture experiments, two *B. bronchiseptica* strains were subcultured together into 10ml of Stainer Sholte media at the appropriate concentrations. The co-culture was incubated at 37°C with continuous agitation. To determine the concentration of each strain in the co-culture at various time points, 100 μ l of the co-culture was serially diluted in PBS and spread on six Bordet-Gengou agar plates, half of which were treated with gentamycin. After two days of incubation at 37°C, the colony forming units (CFU) on each plate were counted to determine the concentrations of each strain at consecutive time points.

The phage-sensitivity of a single BbGm colony was tested by using the standard protocol [16]. The lack of host diversity mechanisms of $\phi\Delta orf5$ was tested at 0 and 48 hours postinoculation by using the standard phage-titering protocol on the lawns of susceptible Bb and Bb Δprn Gm.

APPENDIX B: SPONTANEOUS PHAGE INDUCTION

In vitro evidence of the spontaneous release of phage is provided in Fig. 6. The strain (Bb:: ϕ) carrying the phage and the susceptible strain (BbGm) are co-cultured without exogenous phage. The initial ratio of the strain Bb:: ϕ to the strain BbGm is reversed around 8-10 hours, which is mediated by the phage spontaneously released from the strain Bb:: ϕ . Based on this result, we use spontaneous lysis rate $\delta = 0.054$ for the numerical simulations.

APPENDIX C: DERIVATION OF THE INVASION CRITERIA IN EQS. (2) AND (4)

Our primary model of phage-mediated competition depicted in Fig. 2 is limited to the case where one host is perfectly phage-resistant and the other is phage-susceptible. However in general cases both invading and resident hosts can be susceptible to phage infection but with differential susceptibilities. Here we model the invasion of a host A endogenously and exogenously carrying the phage to another host B. The hosts are characterized by the differential susceptibilities κ_A and κ_B against the phage, and the phage pathology P_A and P_B . We rescale and non-dimensionalize the variables, $i_j =$

$I_j/S_B(0)$, $s_j = S_j/S_B(0)$, $l_j = L_j/S_B(0)$, $\phi = \Phi/S_B(0)$, $n_{max} = N_{max}/S_B(0)$, $\tau = at$, $\alpha = \delta/a$, $\beta = \lambda/a$, and $\gamma_j = \kappa_j S_B(0)/a$ where $j = A, B$. Then we obtain

$$\begin{aligned}\frac{ds_j}{d\tau} &= (1 - n/n_{max} - \gamma_j \phi) s_j \\ \frac{di_j}{d\tau} &= (1 - P_j) \gamma_j \phi s_j + (1 - n/n_{max} - \alpha) i_j \\ \frac{dl_j}{d\tau} &= P_j \gamma_j \phi s_j - \beta l_j \\ \frac{d\phi}{d\tau} &= \chi (\alpha \sum_j i_j + \beta \sum_j l_j) - \sum_j \gamma_j \phi s_j\end{aligned}\quad (C1)$$

where $n = \sum_j (i_j + s_j + l_j)$ and $j = A, B$. The initial conditions for Eq. (C1) are $i_B(0) = l_A(0) = l_B(0) = 0$, $s_B(0) = 1$, $s_A(0) > 0$, $i_A(0) > 0$ and $\phi(0) \geq 0$. The above general model and Eq. (C1) are reduced to the primary model depicted in Fig. 2 and Eq. (1) when $P_A = 0$, $\gamma_A = 0$ and $S_A(0) = 0$.

CASE I: If $\phi(0) = 0$ and $\alpha = 0$, then the 7-dimensional ODE system reduces to

$$\begin{aligned}\frac{ds_j}{d\tau} &= (1 - (\sum_j s_j + i_A)/n_{max}) s_j, \\ \frac{di_A}{d\tau} &= (1 - (\sum_j s_j + i_A)/n_{max}) i_A.\end{aligned}$$

where $j = A, B$ and $i_B(\tau) = l_A(\tau) = l_B(\tau) = 0$ for $\tau > 0$. All populations s_j and i_A will grow with the same growth rate and the initial ratio $i_A(0) : s_A(0) : s_B(0)$ remains unchanged to be $i_A(\tau) : s_A(\tau) : s_B(\tau)$ for all $\tau > 0$. In other words, there will be no pathogen-mediated competition.

CASE II: When $\phi(0) > 0$, we can derive the invasion criteria in Eqs. (2) and (4) in the limit $\gamma_j \rightarrow \infty$ and $\beta \rightarrow \infty$.

CASE II-A: $\tau = 0$ Limit.

An appropriate timescale near $\tau = 0$ is $\sigma = \tau/\epsilon$ where $\epsilon = 1/\beta$. The effect of the transformation $\sigma = \tau/\epsilon$ is to magnify the neighborhood of $\tau = 0$, i.e., for a fixed $0 < \tau \ll 1$, we have $\sigma \gg 1$ as $\epsilon \rightarrow 0$. With the transformations $\sigma = \tau/\epsilon$, $s_j(\tau; \epsilon) = \hat{s}_j(\sigma; \epsilon)$, $i_j(\tau; \epsilon) = \hat{i}_j(\sigma; \epsilon)$, $l_j(\tau; \epsilon) = \hat{l}_j(\sigma; \epsilon)$, $\phi_j(\tau; \epsilon) = \hat{\phi}_j(\sigma; \epsilon)$, $\xi_j = \gamma_j/\beta$, Eq. (C1) become

$$\begin{aligned}\frac{d\hat{s}_j}{d\sigma} &= \epsilon(1 - n/n_{max}) \hat{s}_j - \xi_j \hat{\phi} \hat{s}_j \\ \frac{d\hat{i}_j}{d\sigma} &= (1 - P_j) \hat{\phi} \hat{s}_j \xi_j + \epsilon(1 - n/n_{max} - \alpha) \hat{i}_j \\ \frac{d\hat{l}_j}{d\sigma} &= P_j \hat{\phi} \hat{s}_j \xi_j - \hat{l}_j \\ \frac{d\hat{\phi}}{d\sigma} &= \chi \sum_j \hat{l}_j - \sum_j \xi_j \hat{\phi} \hat{s}_j + \epsilon \chi \alpha \sum_j \hat{i}_j\end{aligned}\quad (C2)$$

In a regular perturbation theory [27] the solutions are expanded in order of ϵ , $\hat{s}_j(\sigma; \epsilon) = \sum_{n=0} \epsilon^n \hat{s}_{j,n}(\sigma)$,

$\hat{i}_j(\sigma; \epsilon) = \sum_{n=0} \epsilon^n \hat{i}_{j,n}(\sigma)$, $\hat{l}_j(\sigma; \epsilon) = \sum_{n=0} \epsilon^n \hat{l}_{j,n}(\sigma)$, $\hat{\phi}(\sigma; \epsilon) = \sum_{n=0} \epsilon^n \hat{\phi}_n(\sigma)$. We now set $\epsilon = 0$ to get 0(1) system,

$$\frac{d\hat{s}_{j,0}}{d\sigma} = -\xi_j \hat{\phi}_0 \hat{s}_{j,0} \quad (C3)$$

$$\frac{d\hat{i}_{j,0}}{d\sigma} = (1 - P_j) \xi_j \hat{\phi}_0 \hat{s}_{j,0} \quad (C4)$$

$$\frac{d\hat{l}_{j,0}}{d\sigma} = P_j \xi_j \hat{\phi}_0 \hat{s}_{j,0} - \hat{l}_{j,0} \quad (C5)$$

$$\frac{d\hat{\phi}_0}{d\sigma} = \chi \sum_j \hat{l}_{j,0} - \sum_j \xi_j \hat{\phi}_0 \hat{s}_{j,0} \quad (C6)$$

with the initial conditions $\hat{i}_{B,0}(0) = \hat{l}_{A,0}(0) = \hat{l}_{B,0}(0) = 0$, $\hat{s}_{B,0}(0) = 1$, $\hat{s}_{A,0}(0) \geq 0$, $\hat{i}_{A,0}(0) > 0$ and $\hat{\phi}_0(0) > 0$.

By integrating Eqs. (C3) and (C4), we obtain

$$\hat{s}_{j,0}(\sigma) = \hat{s}_{j,0}(0) \exp\left(-\int_0^\sigma \xi_j \hat{\phi}_0(x) dx\right), \quad (C7)$$

$$\begin{aligned}\hat{i}_{j,0}(\sigma) &= \hat{i}_{j,0}(0) \\ &+ (1 - P_j) \hat{s}_{j,0}(0) \int_0^\sigma F_j(y) dy\end{aligned} \quad (C8)$$

where $F_j(y) = \xi_j \hat{\phi}_0(y) \exp\left(-\int_0^y \xi_j \hat{\phi}_0(x) dx\right)$. Eqs. (C5) and (C6) can be rewritten

$$\frac{d\hat{l}_{j,0}}{d\sigma} = P_j \hat{s}_{j,0}(0) F_j(\sigma) - \hat{l}_{j,0}(\sigma) \quad (C9)$$

$$\frac{d\hat{\phi}_0}{d\sigma} = \chi \sum_j \hat{l}_{j,0}(\sigma) - \sum_j \hat{s}_{j,0}(0) F_j(\sigma) \quad (C10)$$

Lemma 1. $\hat{\phi}_0(\sigma)$ is strictly positive for $\sigma \geq 0$ if $\hat{\phi}_0(0) > 0$ and $\chi P_j > 1$.

Proof. Let $Z(\sigma) = \hat{\phi}_0(\sigma) + \chi \sum_j \hat{l}_{j,0}(\sigma)$. $Z(0) > 0$ because $\hat{\phi}_0(0) > 0$. Because $\hat{i}_{j,0}(\sigma)$, $\hat{s}_{j,0}(\sigma)$, $\hat{l}_{j,0}(\sigma)$ and $\hat{\phi}_0(\sigma)$ are non-negative for $\sigma \geq 0$, $\frac{dZ}{d\sigma} = \sum_j (\chi P_j - 1) \hat{s}_{j,0}(0) F_j(\sigma) \geq 0$ if $\chi P_j > 1$. Therefore $Z(\sigma)$ is strictly positive and non-decreasing for all $\sigma \geq 0$. Suppose now that there exists $\sigma_o > 0$ such that $\hat{\phi}_0(\sigma) = 0$ for $\sigma > \sigma_o$. Then both $F_j(\sigma)$ and $\hat{l}_{j,0}(\sigma)$ will become zero for $\sigma > \sigma_o$, resulting in $Z(\sigma) = 0$ for $\sigma > \sigma_o$. This contradicts that $Z(\sigma)$ is strictly positive for all $\sigma \geq 0$. Therefore $\hat{\phi}_0(\sigma) > 0$ for all $\sigma \geq 0$. \square

Lemma 2. $F_j(y)$ is strictly positive for $y > 0$ and $F_j(y)$ asymptotically approaches zero as $y \rightarrow \infty$.

Proof. Strict positiveness of $F_j(y)$ for $y > 0$ follows from lemma 1. For the second part, we divide the integration in the exponent into two parts,

$$\int_0^y dx \xi_j \hat{\phi}_0(x) = \int_0^{y-w} dx \xi_j \hat{\phi}_0(x) + \int_{y-w}^y dx \xi_j \hat{\phi}_0(x)$$

where $y \gg 1$ and $w \in (0, y)$ must be such that $\hat{\phi}_0(x)$ is either non-decreasing or non-increasing in the interval $x \in [y - w, y]$. Then there exists $\lambda \in [0, 1]$ such that $\int_{y-w}^y dx \xi_j \hat{\phi}_0(x) = [\lambda \xi_j \hat{\phi}_0(y) + (1 - \lambda) \xi_j \hat{\phi}_0(y - w)]w$. By defining $\hat{\phi}_{min} \equiv \min_{x \geq 0} \hat{\phi}_0(x)$, $\int_0^{y-w} dx \xi_j \hat{\phi}_0(x) \geq (y - w) \xi_j \hat{\phi}_{min}$ and $\int_{y-w}^y dx \xi_j \hat{\phi}_0(x) \geq [\lambda \xi_j \hat{\phi}_0(y) + (1 - \lambda) \xi_j \hat{\phi}_{min}]w$. Then we can obtain

$$\begin{aligned} F_j(y) &= \xi_j \hat{\phi}_0(y) \text{Exp}(-\int_0^y dx \xi_j \hat{\phi}_0(x)) \\ &\leq \xi_j \hat{\phi}_0(y) e^{-\lambda w \xi_j \hat{\phi}_0(y)} e^{-(y-\lambda w) \xi_j \hat{\phi}_{min}} \\ &\leq \frac{1}{\lambda w} e^{-(y-\lambda w) \xi_j \hat{\phi}_{min}-1} \end{aligned}$$

where in the third line we used $xe^{-x} \leq e^{-1}$ for all $x > 0$. As $y \rightarrow \infty$, $F_j(y) \rightarrow 0$. \square

Lemma 3. Let $G_j(\sigma) = \int_0^\sigma F_j(y) dy$. $G_j(\sigma)$ asymptotically approaches 1 as $\sigma \rightarrow \infty$.

Proof.

$$\begin{aligned} G_j(\sigma) &= \int_0^\sigma dy \xi_j \hat{\phi}_0(y) \text{Exp}(-\int_0^y dx \xi_j \hat{\phi}_0(x)) \\ &= \int_0^\sigma dy H_j'(y) e^{-H_j(y)} \\ &= 1 - e^{-H_j(\sigma)} \end{aligned}$$

where $H_j(y) = \int_0^y dx \xi_j \hat{\phi}_0(x)$ and $H_j(0) = 0$. Using $H_j(\sigma) \geq \sigma \xi_j \hat{\phi}_{min}$, $e^{-H_j(\sigma)} \leq e^{-\sigma \xi_j \hat{\phi}_{min}}$ for $\sigma > 0$. As $\sigma \rightarrow \infty$, $e^{-H_j(\sigma)} \rightarrow 0$ and $G_j(\sigma) \rightarrow 1$. \square

Using the above lemmas, we know that both $\hat{s}_{j,0}(\sigma)$ and $\hat{l}_{j,0}(\sigma)$ approaches zero as $\sigma \rightarrow \infty$ while keeping $0 < \tau \ll 1$. In the limit of $\sigma \rightarrow \infty$ we obtain, using Eq. (C8) and initial conditions, $\hat{s}_{B,0}(0) = 1$, $\hat{i}_{B,0}(0) = \hat{l}_{A,0}(0) = \hat{l}_{B,0} = 0$, and

$$\begin{aligned} r_{AB}(\sigma) &= \frac{\hat{i}_{A,0}(\sigma) + \hat{s}_{A,0}(\sigma) + \hat{l}_{A,0}(\sigma)}{\hat{i}_{B,0}(\sigma) + \hat{s}_{B,0}(\sigma) + \hat{l}_{B,0}(\sigma)} \\ &= \frac{(1 - P_A) \hat{s}_{A,0}(0) + \hat{i}_{A,0}(0)}{(1 - P_B)} \end{aligned} \quad (\text{C11})$$

where $r_{AB}(0) = \hat{i}_{A,0}(0) + \hat{s}_{A,0}(0)$. When $\hat{s}_{A,0}(0) \gg \hat{i}_{A,0}(0)$, Eq. (4) is recovered, in the limit of $\gamma_j \rightarrow \infty$, $\beta \rightarrow \infty$ and $\sigma \rightarrow \infty$ while keeping $0 < \tau \ll 1$,

$$r_{AB}(\sigma) = r_{AB}(0)(1 - P_A)/(1 - P_B) \quad (\text{C12})$$

Moreover when $P_A = 0$, $\gamma_A = 0$ and $\hat{s}_{A,0}(0) = 0$, Eq. (2) is recovered, in the limit of $\gamma_B \rightarrow \infty$, $\beta \rightarrow \infty$ and $\sigma \rightarrow \infty$ while keeping $0 < \tau \ll 1$,

$$r_{AB}(\sigma) = r_{AB}(0)/(1 - P_B) \quad (\text{C13})$$

In case II-B we will prove that these ratios in Eqs. (C12) and (C13) remain unchanged in the limit of $\tau = \infty$.

CASE II-B: $\tau = \infty$ limit.

To study the long time limit, we go back to Eq. (C1). Using the quasi-steady state approximation of the third equation in Supporting Eq. (1) $\frac{1}{\beta} \frac{dl_j}{d\tau} = 0 = P_j \phi s_j \gamma_j / \beta - l_j$, in the limit $\gamma_j \rightarrow \infty$ and $\beta \rightarrow \infty$, and $\chi P_j > 1$, we obtain $\frac{d\phi}{d\tau} = \chi \alpha \sum_j i_j + \phi \sum_j (\chi P_j - 1) \gamma_j s_j \geq 0$ for $\tau \gg 1$ (Equality holds when $\alpha = 0$ and $s_j(\tau) = 0$). Because $\phi(\tau)$ is strictly positive and non-decreasing for $\tau \gg 1$ and $\phi \gamma_j \gg 1$, $\frac{ds_j}{d\tau} = (1 - n/n_{max} - \phi \gamma_j) s_j < 0$ for $\tau \gg 1$. Therefore using $l_j(\tau) = P_j \phi \gamma_j s_j(\tau) / \beta$, $s_j(\tau) = l_j(\tau) = 0$ for $\tau \gg 1$. In the limit of $\beta \rightarrow \infty$, $\gamma_j \rightarrow \infty$ and $\tau \gg 1$, Eq. (C1) reduce to the effective three dimensional ODE

$$\begin{aligned} \frac{di_j}{d\tau} &= (1 - \frac{\sum_j i_j}{n_{max}} - \alpha) i_j \\ \frac{d\phi}{d\tau} &= \chi \alpha \sum_j i_j \end{aligned}$$

Note that the first equation for $i_j(\tau)$ is independent of $\phi(\tau)$. Now if $\alpha \geq 1$, $\frac{di_j}{d\tau} < 0$ for $\tau \gg 1$ and $i_j(\infty) = 0$, which means that both A and B populations go extinct. Otherwise if $0 \leq \alpha < 1$, both $i_A(\tau)$ and $i_B(\tau)$ will grow with the same growth rate. Thus the ratio $r_{AB}(\sigma)$, determined in the limit of $\sigma \rightarrow \infty$ while keeping $0 < \tau \ll 1$, remains unchanged in the limit $\tau \gg 1$.

Case III. If $\phi(0) = 0$ and $\alpha > 0$, this is equivalent to case II. Suppose that $\phi(\tau) > 0$ when $\tau > \tau_{min}$ where τ_{min} is the earliest time when the first phage are spontaneously induced. By defining a new time frame $\tau' = \tau - \tau_{min}$ and rescaling all the concentrations by $S_B(\tau_{min})$, case III becomes equivalent to case II.

APPENDIX D: NUMERICAL INVESTIGATION OF THE INVASION CRITERIA FROM EQS. (2) AND (4)

The invasion criteria in Eqs. (2) and (4) are exact in the limit of large infection-induced lysis rate β and contact rate γ with restrictions on $\chi P_j > 1$ and on the spontaneous lysis rate $0 \leq \alpha < 1$. In order to investigate their validity for small β and γ , we performed numerical simulations. First, the linear relationship in Eq. (2) between the phage pathology P and $r_{AB}(0)/r_{AB}(\infty)$ is validated by extensive numerical calculations with 2000 parameter sets where all parameters are selected uniformly from the biologically relevant intervals (see Fig. 7 for detailed information). Note that $\chi P > 1$ is used for numerical calculations. When γ and β are relatively large, i.e., $0.1 < \gamma, \beta < 10$, all data points fall into the linear line $r_{AB}(0)/r_{AB}(\infty) = 1 - P$ as illustrated in Fig. 7. When $0 < \gamma, \beta < 0.1$, the deviation from the linear relationship increases for small phage pathology P . Thus we conclude that the linear relationship in Eq. (2), $r_{AB}(0)/r_{AB}(\infty) = 1 - P$, is robust to parameter variations and valid for small γ and β .

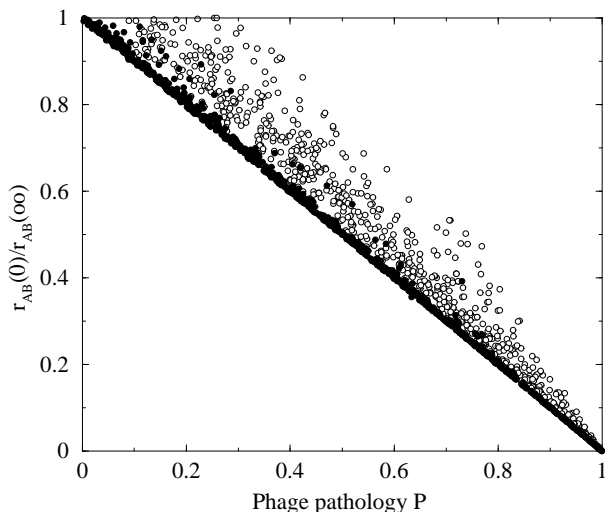


FIG. 7: Numerical verification of the invasion criterion in Eq. (2). A thick solid line is the prediction from Eq. (2). $r_{AB}(0)/r_{AB}(\infty)$ was numerically evaluated by solving Eq. (1) with 2000 sets of parameters chosen uniformly in the intervals $0 < P < 1$ for phage pathology, $1/P < \chi < 100$ for burst size, $0 < \alpha < 0.5$ for normalized spontaneous induction rate, $0 < I_A(0), \phi(0) < 10S_B(0)$ for the initial concentrations of infected bacteria A and phage with respect to the initial concentration of susceptible bacteria B. Filled circles represent the data from 1000 sets of parameters with relatively large γ and β ($0.1 < \gamma, \beta < 10$). Open circles are from another 1000 sets of parameters with small γ and β ($0 < \gamma, \beta < 0.1$).

Second, we also validate the generalized invasion criterion from Eq. (4) numerically with diverse sets of parameters. Fig. 8 shows that the linear relationship in Eq. (4) between $r_{AB}(0)/r_{AB}(\infty)$ and $(1 - P_A)/(1 - P_B)$ is robust against parameter variations. Note that we impose restrictions on $\chi P_j > 1$ and $s_A(0) \gg i_A(0)$ in the nu-

merical calculations. However the linear relationship in Eq. (4) becomes inaccurate when the pathogen is more virulent on the invading population A than on the resident population B, i.e., when P_A is large and P_B is small.

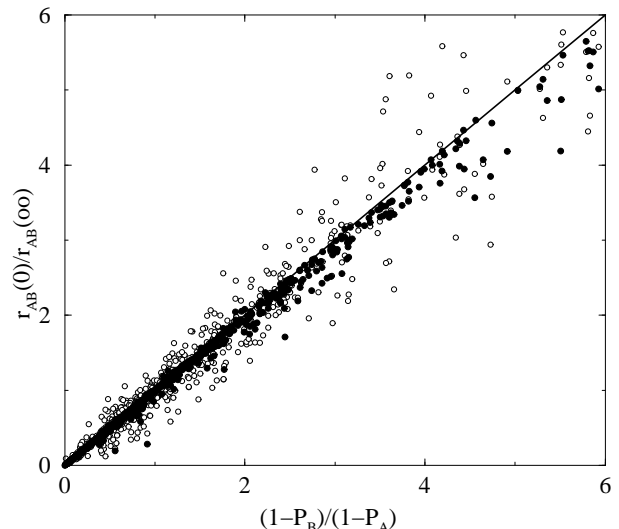


FIG. 8: Numerical verification of the generalized invasion criterion in Eq. (4). $r_{AB}(0)/r_{AB}(\infty)$ was numerically evaluated by solving Eq. (C1) with 2000 sets of parameters chosen uniformly in the intervals $0 < P_A, P_B < 1$ for phage pathologies on the host A and B, $1/\min\{P_A, P_B\} < \chi < 100$ for burst size, $0 < \alpha < 0.5$ for normalized spontaneous induction rate, $10^{-1}S_B(0) < S_A(0) < 10S_B(0)$ and $0 < I_A(0), \phi(0) < 10^{-2}S_B(0)$ for the initial concentrations of susceptible and infected bacteria A and phage. Filled circles represent the data from 1000 sets of parameters with relatively large γ_j and β ($0.1 < \gamma_j, \beta < 10$). Open circles are from another 1000 sets of parameters with small γ_j and β ($0 < \gamma_j, \beta < 0.1$).

-
- [1] R. M. Anderson and R. M. May, *Infectious diseases of humans. Dynamics and control*, Oxford University Press, Oxford, 1991.
 - [2] U. Dickmann, J. A. J. Metz, M. W. Sabelis, and K. Sigmund (Eds.) *Adaptive Dynamics of Infectious Diseases: In Pursuit of Virulence Management*, Cambridge University Press, Cambridge, United Kingdom, 2002.
 - [3] Peter Hudson and Jon Greenman, *TREE*, **13**, 387(1998) and references therein.
 - [4] F. Thomas, M. B. Bonsall and A. P. Dobson, Parasitism, biodiversity and conservation. In: F. Thomas, F. Renaud and J. F. Guegan, editors. *Parasitism and ecosystems*. Oxford University Press, Oxford, 2005.
 - [5] M. B. Bonsall and M. P. Hassell, *Nature*, **388**, 371(1997).
 - [6] T. Park, *Ecol. Monogr.*, **18**, 267(1948).
 - [7] C. E. Mitchell, A. G. Power, *Nature*, **421** 625(2003).
 - [8] M. E. Torchin, K. D. Lafferty, A. P. Dobson, V. J. McKenzie and A. M. Kuris, *Nature*, **421** 628(2003).
 - [9] S. Hedrick, *Immunity*, **21**, 607(2004).
 - [10] R. M. May and R. M. Anderson, *Proc. Roy. Soc. Lond. B*, **219**, 281(1983).
 - [11] F. Fenner and G. M. Woodroffe, *Australian Journal of Experimental Biology and Medicine*, **43**, 359(1965).
 - [12] N. T. J. Bailey, *The mathematical theory of infectious diseases and its applications*, Griffin, High Wycombe, 1975.
 - [13] H. N. Simpson, *Invisible armies. The impact of disease on American history*, The Bobbs-Merrill Company, Indianapolis, IN, 1980.
 - [14] B. J. M. Bohannan and R. E. Lenski, *Ecology Letters*, **3**, 362(2000).
 - [15] B. J. M. Bohannan and R. E. Lenski, *Am. Nat.*, **156**, 329(2002).
 - [16] M. Lui *et al*, *Science*, **295**, 2091(2002).
 - [17] M. Lui *et al*, *J. Bacteriol.*, **186**, 1503(2004).
 - [18] M. Ptashne, *A Genetic Switch*, Cell Press and Blackwell

Scientific Publications, Cambridge, MA, 1992.

- [19] R. D. Holt and J. H. Lawton, *Annu. Rev. Ecol. Syst.*, **25**, 495(1994).
- [20] R. D. Holt and J. Pickering, *Am. Nat.*, **125**, 196(1985).
- [21] M. Begon et al, *Am. Nat.*, **139**, 1131(1992).
- [22] R. G. Bowers and J. Turner, *J. Theor. Biol.*, **187**, 95(1997).
- [23] J. V. Greenman and P. J. Hudson, *J. Theor. Biol.*, **185**, 345(1997).
- [24] J. M. Mahaffy, Marine phage-host interactions in a two-compartment model, poster presented at the 2004 SIAM Conference of the Life Sciences, July 13 2004.
- [25] S. Doulatov *et al*, *Nature*, **431**, 476(2004).
- [26] O. Restif and J. Koella, *Am. Nat.*, **164**, E90(2004).
- [27] J. D. Murray, *Mathematical Biology*, Springer-Verlag, New York(1980).